Food and Chemical Toxicology 132 (2019) 110600

Contents lists available at ScienceDirect

Food and Chemical Toxicology

journal homepage: www.elsevier.com/locate/foodchemtox

Short communication

Hepatic and renal tissue damage in Balb/c mice exposed to diisodecyl phthalate: The role of oxidative stress pathways

Yingying Chen[a,b], Chongyao Li[a,b], Peng Song[a,b], Biao Yan[a], Xu Yang[a], Yang Wu[a,*], Ping Ma[a,**]

[a] Laboratory of Environment- Immunological and Neurological Diseases, School of Basic Medical Sciences, Hubei University of Science and Technology, Xianning, 437100, China

[b] School of Pharmacy, Hubei University of Science and Technology, Xianning, 437100, China

ARTICLE INFO

Keywords:
Diisononyl phthalate
Oxidative stress
Hepatic
Renal

ABSTRACT

Diisononyl phthalate (DIDP) is commonly used as a plasticizer in industrial and consumer products, however, its toxicity remains unclear. This study investigated the possible involvement of oxidative stress in DIDP-induced liver and kidney toxicity. Liver function and kidney function, tissue lesions, oxidative stress biomarkers, inflammatory mediators and apoptosis factors were investigated in this study. The results showed that oral exposure to DIDP induced a marked increase in lever of alanine aminotransferase (ALT), aspartate aminotransferase (AST), urinary nitrogen (UREA) and creatinine (CREA), decrease in albumin (ALB) level, as well as causing hepatic and renal histopathological change. Investigation of the role of oxidative stress pathways showed that DBP exposure could lead to a significant increase in levels of reactive oxygen species (ROS), malondialdehyde (MDA), 8-hydroxy-2-deoxyguanosine (8-OHdG), interleukin-1β (IL-1β), tumor necrosis factor-α (TNF-α) and nuclear factor-κB (NF-κB), while a decrease in glutathione (GSH) levels were observed. Administration of vitamin E to DIDP-treated mice restored these biochemical parameters to within normal levels, and resulted in less damage to livers and kidneys. Overall, these results suggest that the oxidative stress pathway is involved in DIDP-induced toxicity.

1. Introduction

Diisodecyl phthalate (DIDP) is commonly used as a plasticizer, with many applications in industrial and consumer products, including but not limited to food wrap, building materials and toys (Morse, 2011; Saravanabhavan and Murray, 2012). DIDP molecules are easily emitted from materials since they are not tightly bound to the polymer matrix (Halden, 2010). A previous study reported that the concentration of DIDP in dust is 73 mg/kg, in soil is 0.007 mg/kg, and in indoor air is 2.8 ng/m^3 (Wormuth et al., 2006). Some studies have already shown that products containing DIDP can result in human exposure, primarily via dermal, oral and inhalation routes, with oral contact being the main exposure route for humans, particularly for children (Bradley et al., 2013; Giovanoulis et al., 2018). It is therefore important to study any potential toxic effects of DIDP *in vivo*.

DIDP is not known to affect the reproductive system nor to affect development (Chen et al., 2014; Patyna et al., 2006). However, the potential for DIDP to affect the liver and kidney has received considerable critical attention, since DIDP predominantly distributes to these organs after oral ingestion (Saravanabhavan and Murray, 2012). Cho et al. reported that higher doses of DIDP can reduce the weigh and longevity of rats, and can result in the enlargement of theirs livers and kidneys (Cho et al., 2008). There is emerging evidence that exposure to DIDP may result in a higher number of hepatocellular adenomas in the male rasH2 mice (Cho et al., 2011). To date, the mechanisms behind DIDP-induced liver and kidney damage remains poorly understood.

Previous studies have reported that the toxicity induced by DIDP may be attributed to the enhanced production of reactive oxygen species (ROS), which in turn results in oxidative stress (Qin et al., 2018; Shen et al., 2017). At high concentrations, ROS can be notable mediators of damage to cell macromolecules, such as lipids, membranes, proteins and nucleic acids (Valko et al., 2006; Ma et al., 2013; Feng et al., 2013a). These alterations probably transform cell function, and eventually lead to tissue lesions and cell apoptosis (Majhi et al., 2011; Feng et al., 2013b, 2015). Injuries occur in various organs, including the liver and kidney, and toxic reactions are known to be involved in inflammation, fatty liver disease, and diabetic kidney disease (Barcelos et al., 2017; Paradies et al., 2014; Jha et al., 2016). However, there is

* Corresponding author. School of Basic Medical Science, Hubei University of Science and Technology, Xianning, 437100, China.
** Corresponding author. School of Basic Medical Science, Hubei University of Science and Technology, Xianning, 437100, China.
E-mail addresses: wysj2007@126.com (Y. Wu), mping68@126.com (P. Ma).

https://doi.org/10.1016/j.fct.2019.110600
Received 23 February 2019; Received in revised form 16 June 2019; Accepted 19 June 2019
Available online 20 June 2019

very little research into the possible involvement of oxidative stress in DIDP-induced liver and kidney damage.

We hypothesized that DIDP exposure could lead to oxidative damage in hepatic and renal tissues. In this study, Balb/c mice were orally exposed to DIDP for 14 consecutive days. Liver function was assessed by examining levels of alanine aminotransferase (ALT), aspartate aminotransferase (AST) and albumin (ALB). Kidney function was evaluated by measuring urinary nitrogen (UREA) and creatinine (CREA) levels. Hepatic and renal tissue lesions were observed using Hematoxylin-eosin (H&E) staining. Oxidative stress was indicated by ROS, glutathione (GSH), malondialdehyde (MDA) and 8-hydroxy-2-deoxyguanosine (8-OH-dG) levels. Inflammatory mediators were determined by measuring the levels of interleukin-1β (IL-1β), tumor necrosis factor-α (TNF-α) and Nuclear factor-κB (NF-κB). Cell apoptosis was evaluated by examining levels of cysteine-aspartic acid protease 3 (caspase-3), and by observation after Hoechst 33258 staining. Additionally, we evaluated the antioxidant effect of administering Vitamin E, by looking at the levels of oxidative stress. Such changes may have implications for the care of people accidently exposed to DIDP.

2. Materials and methods

2.1. Animal care and ethics statement

5-6 week-old SPF male Balb/c mice were purchased from the Hubei Province Experimental Animal Center (Wuhan, China)All mice were housed in pathogen-free cages at 24–26 °C and 12 h light-dark cycle with 55%–75% humidity. A commercial diet and filtered water was provided *ad libitum*. Mice were quarantined for at least 7 days prior to commencing the study. All animal experiments were conducted in accordance with the National Institutes of Health Guide for the Care and Use of Laboratory Animals, and were approved by the Office of Scientific Research Management of Hubei University of Science and Technology (Xianning, China) with a Certificate approval ID: HBUST-IACUC-2018-001.

2.2. Reagents and kits

DIDP (> 99%), 2′7′-dichlordihydrofluorescein (DCFH-DA), 2-thiobarbituric acid (TBA), hematoxylin and eosin, Hoechst 33258 and Vitamin E were purchased from Sigma- Aldrich (St. Louis, MO, USA). Tween-80 was purchased from Amresco (Solon, OH, USA). Mouse ELISA kits for 8-OHdG, TNF-α, IL-1β and caspase-3 were purchased from eBioscience (San Diego, CA, USA). A colorimetric kit for glutathione (GSH) and a Folin-phenol reagent kit were purchased from Jiancheng Bioengineering Institute (Nanjing, China). Colorimetric kits for alanine aminotransferase (ALT), aspartate aminotransferase (AST), albumin (ALB), urinary nitrogen (UREA) and creatinine (CREA) were purchased from iCubio Biomedical Technology (Shenzhen, China). All other chemicals were of the highest grade commercially available.

2.3. Chemical exposure and experimental groups

The acceptable daily intake (ADI) of DIDP is considered to be 0.15 mg/kg/d, a figure proposed by the United States Consumer Products Safety Commission in 2010 (Kransler et al., 2013). Based on this, we chose DIDP exposure concentrations of 0.15, 1.5, 15, 150 mg/kg/d for our experiment. Animals were divided randomly into seven groups of eight mice each, and treated for 14 consecutive days as follows: Saline group; 0.15 mg/kg/d DIDP group (DIDP 0.15); 1.5 mg/kg/d DIDP group (DIDP 1.5); 15 mg/kg/d DIDP group (DIDP 15); 150 mg/kg/d DIDP group (DIDP 150); 150 mg/kg/d DIDP + 100 mg/kg/d Vitamins E group (DIDP150 + Vit E100); 100 mg/kg/d Vitamins E group (Vit E100).

Different concentrations of DIDP were prepared in Tween-80 (1:1 v/v) and diluted with sterile saline for oral administration. The concentration of Tween 80 used in our experiments has been shown in previous *in vivo* pharmacological experiments to be inert, and to have no toxic side effects on the organism (Dimitrov et al., 2011). Therefore, the negative control group was given only saline. The VitE dose level was selected based on daily VitE ingestion in normal human life. The dose of VitE administered was chosen to be 100 mg/kg/d according to Yousef et al. (2006). DIDP and VitE were administered via gavage at the same time every day, After 14 days, all mice were anesthetized intraperitoneally with pentobarbital sodium (100 mg/kg bw). Serum samples were then extracted from heart blood by centrifugation (3000 rpm at 4 °C for 15 min) and stored at −70 °C. Livers and kidneys were removed for tissue sectioning and for the preparation of a homogenate.

2.4. Liver and kidney function

The serum levels of ALT, AST, and ALB for liver function, and UREA and CREA for kidney function, were determined by using appropriate kits according to the manufacturer's instructions. The OD values were obtained using an automatic biochemical analyzer iMagic-V7 (iCubio Biomedical Technology, Shenzhen, China).

2.5. Hematoxylin-eosin staining

The hepatic and renal tissues were collected and fixed in 10% paraformaldehyde solution for 24 h at room temperature, after which they were embedded in paraffin and sectioned into 5 μm slices for Hematoxylin-eosin staining. Each section was observed using a DP73 microscope (Olympus, Tokyo, Japan). Tissue sections were examined qualitatively by two experienced pathologists in a blinded fashion.

2.6. Preparation of tissue homogenates

The hepatic and renal tissues were placed in 10 mL/g ice-cold 1 PBS (pH 7.5) and homogenized using a glass homogenizer. This homogenate was centrifuged at 9800 g for 10 min at 4 °C, and the supernatant collected and kept frozen at −70 °C until needed. The protein concentration of the supernatant was determined using a Folin-phenol assay.

2.7. ROS, GSH and MDA assay

ROS levels in the supernatant were determined by using a general ROS indicator, DCFH-DA, as previously described (Lebel et al., 1992). The supernatant was diluted 50-fold with PBS (pH = 7.5), then 100 μL of the dilution was transferred to a 96-well microplate, and 100 μL of 10 μmol·L-1 DCFH-DA fluorescent dye was added. This was incubated in the dark at 37 °C for 30 min. Fluorescence intensity was measured at an excitation wavelength of 488 nm and an emission wavelength of 525 nm using a fluorescence reader (Hide Chameleon V, Hidex, Finland).

GSH is a major scavenger of ROS in tissues. The GSH concentration in the supernatant was measured using a kit in strict accordance with the manufacturer's instructions. Samples were analyzed using a microplate reader to measure absorbance at 405 nm. GSH levels were calculated according to the formula: GSH (μmol·g-1 prot) = [(measure OD405 – blank OD405)/(standard OD405 - blank OD405)] × standard concentration × sample dilution factor/homogenate protein concentration.

MDA is a typical biomarker for evaluating lipid peroxidation injury. MDA concentration in the brain supernatant was determined using the thiobarbituric acid (TBA) method (Draper and Hadley, 1990). A 0.5 mL sample was added to 2 mL of 0.6% TBA solution and allowed to react in boiling water for 15 min. After cooling with cold water, the mixtures were centrifuged at 9800 g for 10 min at 4 °C, and the supernatant collected to measure absorbance at 532, 600 and 450 nm. MDA levels were obtained according to the formula: MDA (μmol·g-1

prot) = [6.45(OD532-OD600) - 0.56 × OD450]/homogenate protein concentration.

2.8. ELISA assay

Levels of 8-OH-dG, IL-1β, TNF-α and caspase-3 in liver and kidney supernatants were measured using ELISA kits. All procedures were conducted according to the manufacturer's instructions. Concentrations were determined in duplicate for each sample. The sensitivities of the kits were 8 pg/mL for TNF-α, 80 pg/mL for IL-1β, and 1 pg/mL for NF-κB and caspase-3.

2.9. Immunohistochemistry

Sections of tissue were incubated with 3% hydrogen peroxide (H_2O_2) and blocked using an appropriate normal serum of endogenous peroxides. The sections were then boiled in sodium citrate (0.01 mol/L, pH 9.0) for antigen retrieval to unmask the antigen epitopes, permeabilized with 0.2% Triton X-100 for 10 min, and blocked with 5% bovine serum albumin (BSA) in phosphate buffer saline (PBS, PH = 7.4) for 30 min at room temperature. Sections were then incubated at 4 °C overnight with the monoclonal primary antibodies: mouse anti–NF–κB-antibodies (Abcam, Cambridge, USA). Slides were washed with PBS, incubated with secondary antibodies for 30 min at 37 °C and detected with a rabbit IgG peroxidase conjugated streptavidin-biotin complex (SABC-POD) kit, followed by incubation with a diaminobenzidine (DAB) kit. Immunostained sections were viewed under a DP73 microscope. The staining intensity was determined as the average optical density using Image-Pro Plus 6.0 software (Media Cybernetics, Bethesda, MD, USA). A non-stained region was selected and set as the background. All tissue sections were examined qualitatively by two experienced pathologists in a blinded fashion.

2.10. Hoechst 33258 staining

Hoechst 33258 staining was performed to capture apoptotic induction of cells. Tissue sections were washed 3 times with PBS, then stained with Hoechst 33258 solution and kept in the dark for 5 min at room temperature. Sections were again washed 3 times with PBS and immediately imaged using a DP73 fluorescence microscope (Olympus, Tokyo, Japan).

2.11. Statistical analysis

Data are presented as the mean ± standard deviation (SD). A one-way ANOVA followed by an LSD *t*-test was used to compare the differences between groups. A p value < 0.05 was considered significantly different. Data analyses were carried out using IBM SPSS Advanced Statistics 20 (IBM, Armonk, NY, USA). Statistical graphs were generated using GraphPad Prism 6.0 (GraphPad, San Diego, CA, USA).

3. Results

3.1. DIDP treatment resulted in liver and kidney dysfunction

When compared with the saline group, the DIDP150 group demonstrated an increase in ALT content ($p < 0.05$) (Fig. 1A), and the DIDP15 and DIDP150 groups showed a decrease in AST content ($p < 0.05$) (Fig. 1C). A decrease in ALB was found in the serum from the DIDP150 group ($p < 0.01$) (Fig. 1E). The ALT levels of the DIDP150 + VitE100 group were significantly lower than the DIDP150 group ($p < 0.05$) (Fig. 1B and D). Administering vitamin E alongside DIDP reversed the decrease in the levels of ALB that were seen in the DIDP150 group ($p < 0.05$) (Fig. 1F).

An increase in CREA was found in the serum of the DIDP15 group ($p < 0.05$) (Fig. 1G). The level of UREA in the serum from the DIDP150 group was significantly higher than that in the saline group ($p < 0.01$) (Fig. 1I). Vitamin E administered to mice exposed to DIDP significantly attenuated the levels of CREA and UREA compared with levels in the DIDP150 group (CREA: $p < 0.05$, UREA: $p < 0.01$) (Fig. 1H and J).

3.2. DIDP treatment resulted in histopathological changes

Mice suffered greater hepatic damage with increasing DIDP doses. Liver cords broadened, cells expanded, and liver sinuses contracted extensively in the DIDP15 group. At the DIDP150 exposure dose, the liver slices became fuzzy and edematous with extremely loose cytoplasm. The DIDP150 + VitE100 group showed improvement with regard to cell morphology and slight residual edema of the cytoplasm of epithelial cells (Fig. 2A).

Kidney sections also showed signs of damage. A large reduction of tubular space and extreme edema of epithelial cells in the glomeruli were observed, with increasing damage observed from the DIDP15 and DIDP150 group. The DIDP150 + VitE100 group showed marked improvement in the kidney tissues (Fig. 2B).

3.3. DIDP treatment resulted in oxidative damage

After DIDP exposure, the ROS concentration in the DIDP150 group was markedly higher than that in the control group ($p < 0.01$) (Fig. 3A). Similarly, an increase in ROS was found in kidney tissues from the DIDP1.5 group ($p < 0.05$) (Fig. 3C). There was a significant reduction in GSH levels in the liver and kidney tissues of the DIDP150 group ($p < 0.01$) (Fig. 3E and G). The DIDP150 + VitE100 group showed a significant improvement in ROS and GSH levels in liver and kidney tissues compared with the DIDP150 group ($p < 0.05$ and $p < 0.01$) (Fig. 3B, D, 3F and 3H).

An increase in the DIDP exposure dose was associated with an increase in MDA levels in the liver tissues of the DIDP150 group ($p < 0.01$) (Fig. 4A). A significant increase in 8-OH-dG levels was found in the liver tissues of the DIDP150 group ($p < 0.01$) (Fig. 4E). Similar changes were noted for kidney tissues in the DIDP150 group ($p < 0.01$) (Fig. 4C and G). Administering VitE in conjunction with DIDP reversed the increase in MDA levels in liver and kidney tissues seen in the DIDP150 group ($p < 0.05$) (Fig. 4B and D). And VitE together with DIDP significantly attenuated levels of 8-OH-dG compared with those seen in the DIDP150 group ($p < 0.01$) (Fig. 4F and H).

3.4. DIDP treatment induced inflammation and apoptosis

An increase in IL-1β levels was found in the liver tissue of the DIDP15 and DIDP150 mg/kg groups ($p < 0.01$) (Fig. 5A), whereas the were IL-1β levels only higher in the kidney tissue of the DIDP150 group ($p < 0.01$) (Fig. 5C). Similarly, an increase in TNF-α was found in liver and kidney tissues of the DIDP15 group ($p < 0.05$) (Fig. 5E and G). VitE, together with DIDP significantly attenuated the levels of IL-1β and TNF-α compared with those seen in the DIDP150 group ($p < 0.05$) (Fig. 5B, D, 5F and 5H).

A significant increase in NF-κB levels was found in the liver tissue of the DIDP0.15 group (Fig. 6A and B) and in the kidney tissue of the DIDP1.5 group (Fig. 6D and E). There is a significant decrease in NF-κB levels in liver tissue ($p < 0.05$), and kidney tissue ($p < 0.01$) in the DIDP150 + VitE100 group, compared with the DIDP150 exposure group (Fig. 6A, C, 6D and 6F).

A significant increase in caspase-3 levels in both liver and kidney tissues was found in the DIDP150 group ($p < 0.01$) (Fig. 7A and C). Supplementing the DIDP dose with VitE significantly decreased levels of caspase-3 compared with those seen in the DIDP150 group ($p < 0.05$) (Fig. 7B and D). As the dose of DIDP increased, the nucleus began to shrink, and the apoptotic nucleus increased significantly. The highest number of apoptotic bodies was observed in the liver and kidney cells of

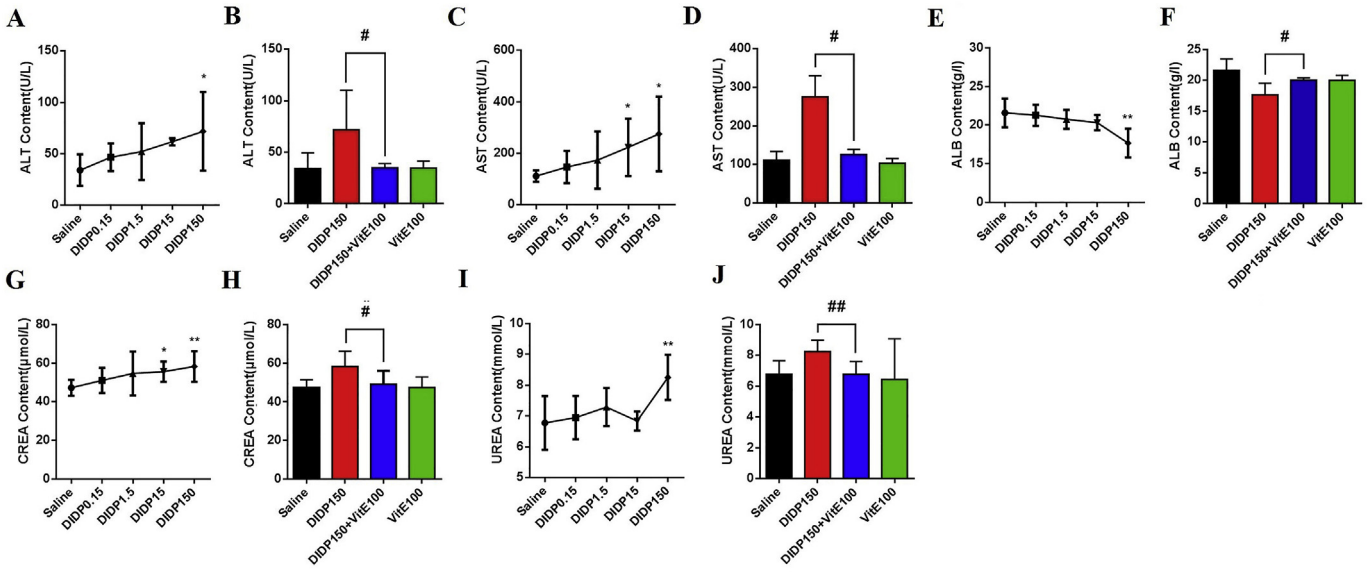

Fig. 1. Liver function and kidney function (A) and (B): ALT level in serum, (C) and (D): AST level in serum, (E) and (F): ALB level in serum, (G) and (H): CREA level in serum, (I) and (J): UREA level in serum. Group data were expressed as mean ± standard deviation (SD), n = 8.*: $p < 0.05$, **: $p < 0.01$, compared with the saline group; #: $p < 0.05$, ##: $p < 0.01$, compared with the DIDP150 group.

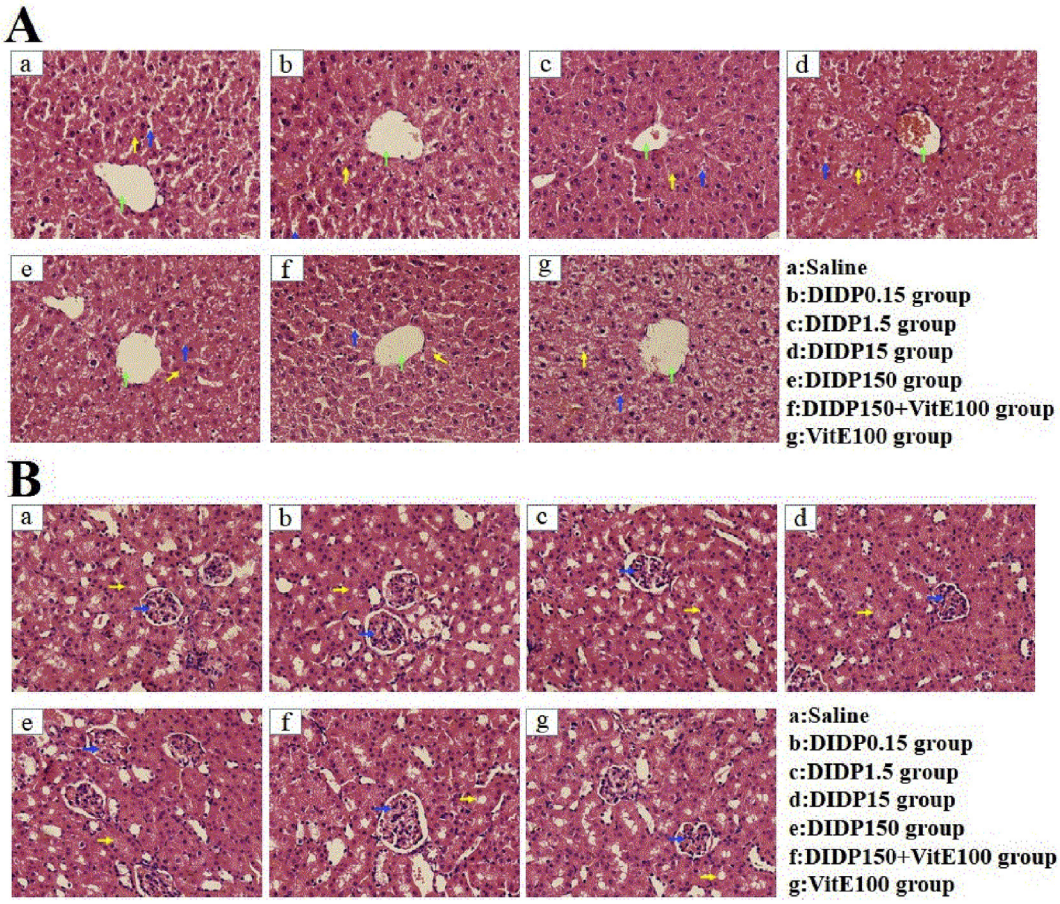

Fig. 2. Liver and Kidney histology (A) shows liver slices: liver cord (yellow arrow), liver sinusoid (blue arrow) and liver cell (green arrow); (B) shows kidney slices: glomerulus (blue arrow) and tubule lumen (yellow arrow); Magnification of × 40. Panel: (a) Saline group; (b) DIDP0.15 group; (c) DIDP1.5 group; (d) DIDP15 group; (e) DIDP150 group; (f) DIDP150 + VitE100 group; and (g) VitE100 group. (n = 8). (For interpretation of the references to color in this figure legend, the reader is referred to the Web version of this article.)

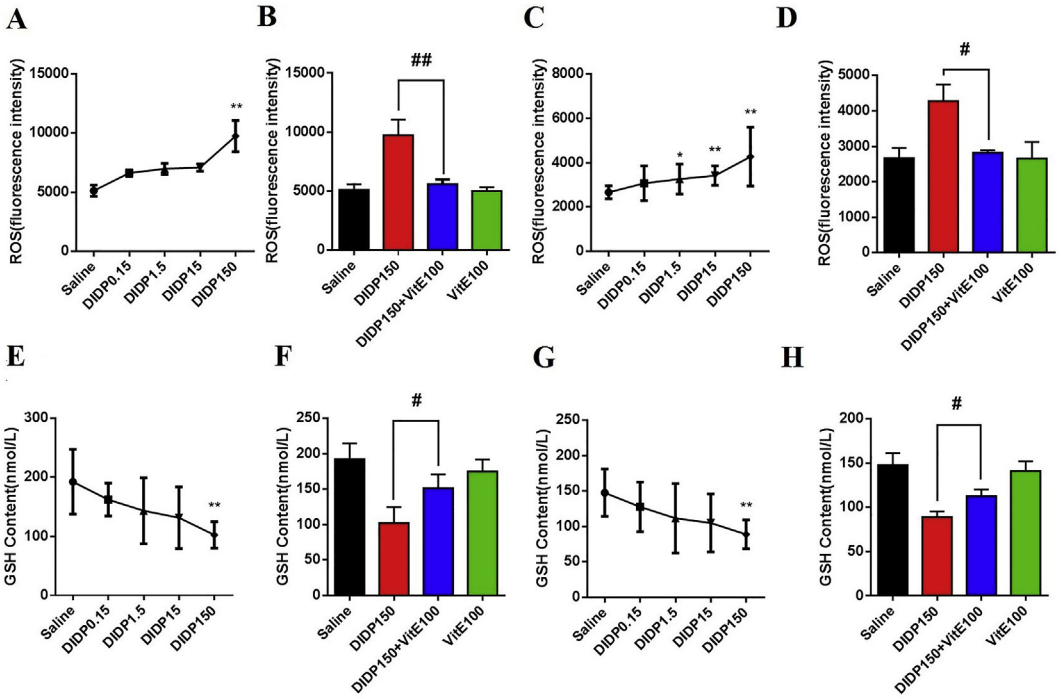

Fig. 3. ROS and GSH levels (A) and (B): ROS levels in the liver, (C) and (D): ROS levels in the kidney, (E) and (F): GSH levels in the liver, (G) and (H): GSH levels in the kidney. Group data were expressed as mean ± SD, n = 8. *: $p < 0.05$, **: $p < 0.01$, compared with the saline group; #: $p < 0.05$, ##: $p < 0.01$, compared with the DIDP150 group.

the DIDP150 group. When mice were treated with VitE, the number of apoptotic nuclei in these cells was reduced (Fig. 7E and F).

4. Discussion

The primary aim of this study was to investigate the possible involvement of oxidative stress in DIDP-induced liver and kidney toxicity. We first used liver function and kidney function to reflect the damage to liver and kidney cells. The function of ALT is to convert alanine into pyruvate, a necessary intermediary in cellular energy production. When the liver is damaged, ALT is released into the blood, usually before obvious signs of liver damage, such as jaundice, occurs

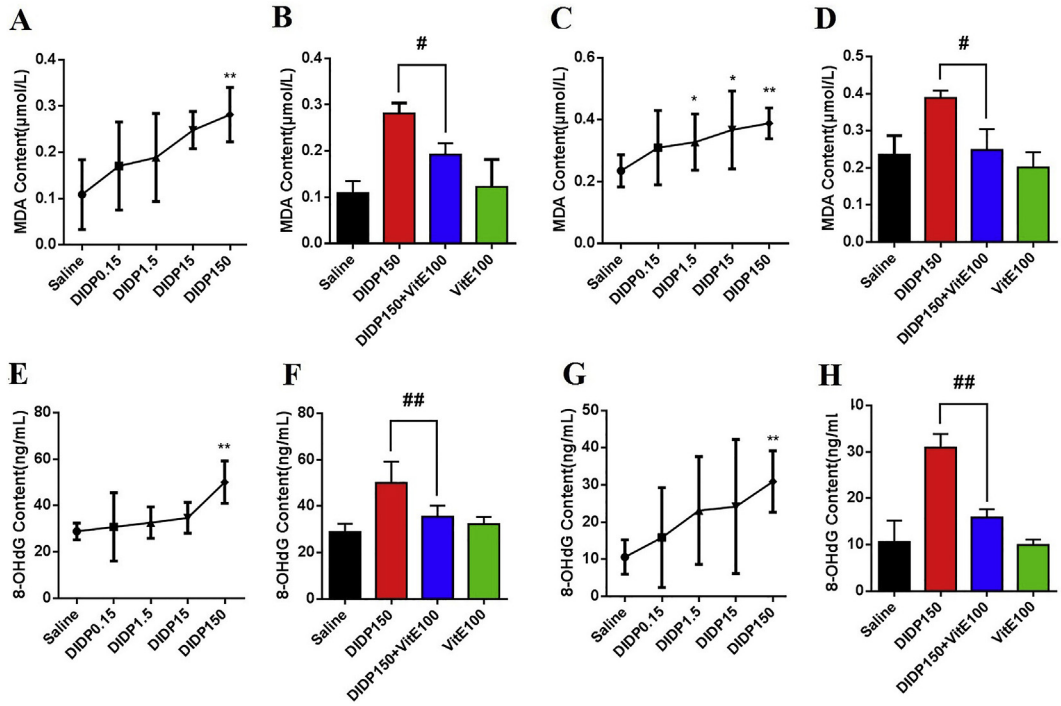

Fig. 4. MDA and 8-OHdG levels (A) and (B): MDA levels in the liver, (C) and (D): MDA levels in the kidney, (E) and (F): 8-OHdG levels in the liver, (G) and (H): 8-OHdG levels in the kidney. Group data were expressed as mean ± SD, n = 8.*: $p < 0.05$, **: $p < 0.01$, compared with the saline group; #: $p < 0.05$, ##: $p < 0.01$, compared with the DIDP150 group.

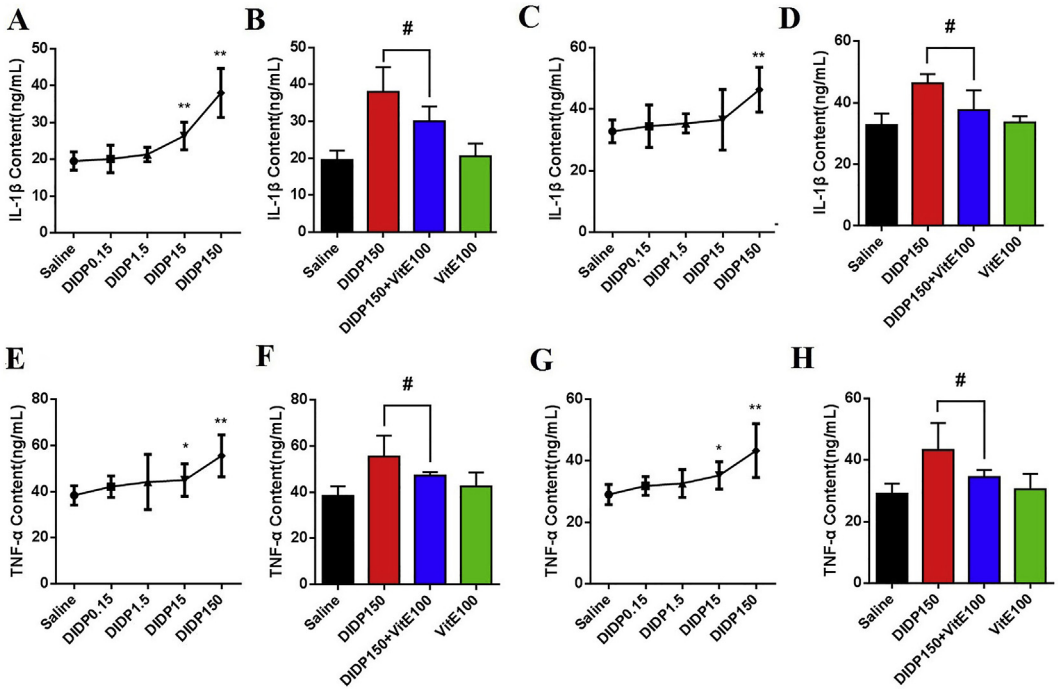

Fig. 5. IL-1β and TNF-α levels (A) and (B): IL-1β levels in the liver, (C) and (D): IL-1β levels in the kidney, (E) and (F): TNF-α levels in the liver, (G) and (H): TNF-α levels in the kidney. Group data were expressed as mean ± SD, n = 8. *: $p < 0.05$, **: $p < 0.01$, compared with the saline group; #: $p < 0.05$, ##: $p < 0.01$, compared with the DIDP150 group.

(Nian et al., 2019). When the liver damage worsens, the mitochondria are destroyed, and a large quantity of AST is released, resulting in a marked increase in serum AST levels (Hoekstra et al., 2013). Serum ALB is the most abundant blood plasma protein and is produced in the liver. It comprises a large proportion of all plasma protein. Low ALB levels may be the result of liver disease (Nian et al., 2019). The kidneys excrete CREA and UREA, so CREA and UREA levels are important indicators for evaluating renal function (Binnenmars et al., 2017). Our study demonstrated that DIDP exposure enhanced ALT, AST, CREA and UREA levels, resulting in liver and kidney damage in the DIDP150 group.

This study provides evidence of changes in the histoarchitecture of

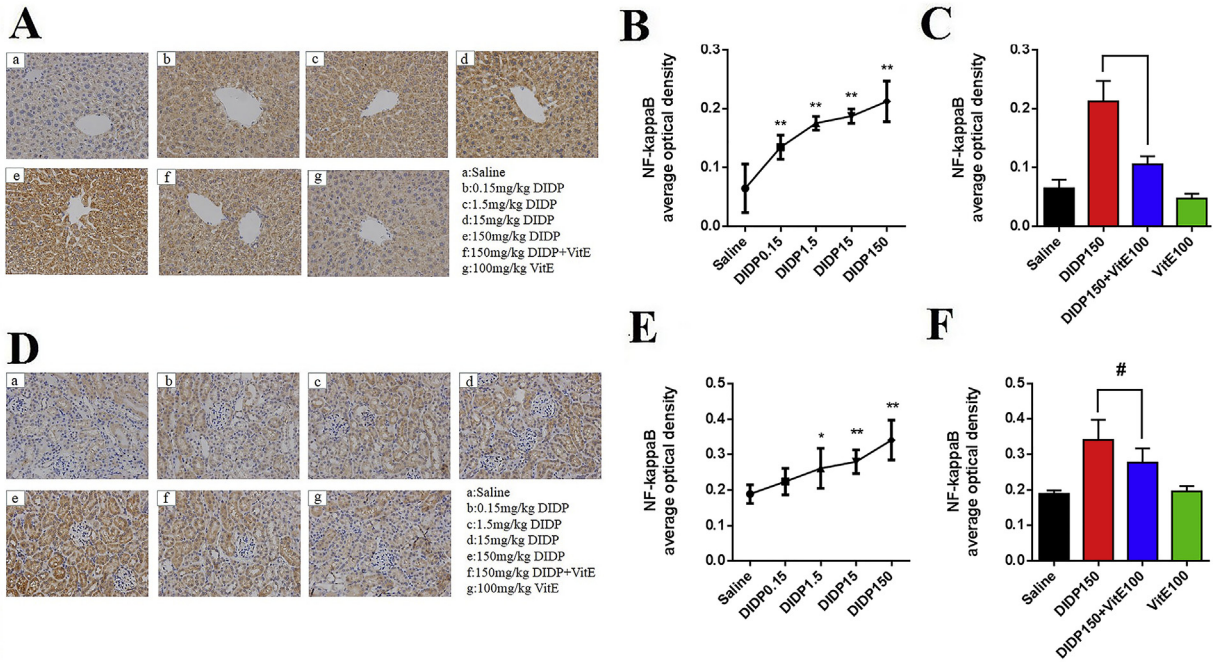

Fig. 6. NF-κB levels (A) Immunohistochemistry for NF-κB in the liver, (B) and (C) average optical density for NF-κB in the liver, (D) Immunohistochemistry for NF-κB in the kidney, (E) and (F) average optical density for NF-κB in the kidney. Magnification × 40. Panel: (a) Saline group; (b) DIDP0.15 group; (c) DIDP1.5 group; (d) DIDP15 group; (e) DIDP150 group; (f) DIDP150 + Vit E100 group; and (g) VitE100 group. Group data were expressed as mean ± SD, n = 8.*: $p < 0.05$, **: $p < 0.01$, compared with the saline group; #: $p < 0.05$, ##: $p < 0.01$, compared with the DIDP150 group.

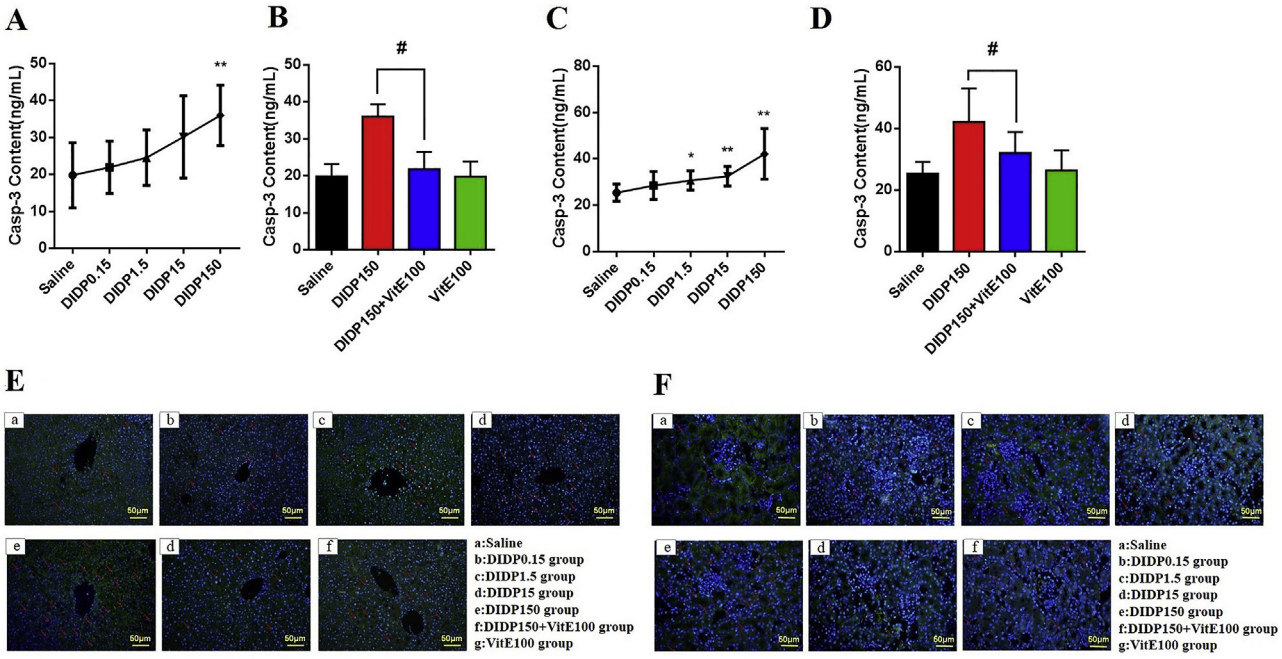

Fig. 7. Caspase-3 levels and Hoechst 33258 staining (A) and (B): Caspase-3 levels in the liver, (C) and (D): Caspase-3 levels in the kidney. Group data were expressed as mean ± SD, n = 8. **: $p < 0.01$, compared with the saline group; #: $p < 0.05$, compared with the DIDP150 group, (E) liver tissue and (F) kidney tissue after Hoechst 33258 staining: apoptotic body (red arrow). Panel: (a) Saline group; (b) DIDP0.15 group; (c) DIDP1.5 group; (d) DIDP15 group; (e) DIDP150 group; (f) DIDP150 + VitE100 group; and (g) VitE100 group. (n = 8). (For interpretation of the references to color in this figure legend, the reader is referred to the Web version of this article.)

the liver and kidney in response to DIDP. At the highest exposure dosage, the liver slices were fuzzy and edemic, with an extremely loose cytoplasm. A large reduction in the tubular space and extreme edema of epithelial cells in the glomeruli were observed in kidney slices. These general changes can result in chronic hepatic or renal diseases. The visible tissue injury clearly shows that several cells have been damaged.

An imbalance between the production of ROS and antioxidant defenses can cause oxidative stress. ROS are key players in oxidative stress, and are the products of cellular metabolism, primarily in the mitochondria (Rimessi et al., 2016). Oxidative stress can result in glutathione depletion, lipid peroxidation, membrane damage, DNA strand breaks, and the activation of proteases, nucleases, and protein kinases. The most extensively studied DNA lesion is the formation of 8-OH-dG. This oxidized DNA product is important because it is a good biomarker of the oxidative stress in an organism, and is a potential biomarker of carcinogenesis (Espinosadiez et al., 2015). Our data suggest a dosage–response relationship that is in agreement with the trends indicated by the results obtained from the ROS, MDA, GSH, and 8-OHdG tests that show that DIDP increases levels of oxidative stress and/or leads to oxidative damage in various tissues and cells.

In addition, ROS have been reported to be involved in signal transduction pathways (Espinosadiez et al., 2015) and can induce apoptosis or necrosis, which may ultimately lead to organ dysfunction and even death. Proinflammatory cytokines, such as IL-1β and TNF-α, were determined in this study because these cytokines are associated with oxidative stress (Chen et al., 2013). NF-κB is a key mediator of TNF-α responses and is thus an attractive target for therapeutic intervention against inflammatory diseases (Wu and Zhou, 2010). In this study, we observed statistically significant increases in IL-1β, NF-κB and TNF-α production due to exposure to higher concentrations of DIDP, and this trend is similar to that seen in the analysis of oxidative damage. Caspase-3 is considered to be the most critical of the executioner caspases in the process of apoptosis, and its activation is often used as an important indicator of apoptosis (Choudhary et al., 2015). Hoechst 33258 staining is used to visualize nuclear changes and apoptotic body formations that are characteristic of apoptosis. Cells are considered as apoptotic if their nuclei present chromatin condensation or nuclear beading (Kasibhatla and Amarantemendes, 2006). We observed significant caspase-3 activation and aggregation of apoptotic bodies in the liver and kidneys of the DIDP150 group, which is indicative of apoptosis.

VitE is a powerful antioxidant that works in aqueous environments in the body. Our study showed that treatment with the antioxidant VitE prevented the DIDP-induced liver and kidney damage, reduced ROS generation, GSH depletion, lipid peroxidation, DNA damage, reversed liver and kidney dysfunction, decreased pro-inflammatory cytokine IL-1β, TNF-α and NF-κB levels, and improved aggregation of apoptotic nuclei and expression of caspase-3. Oral DIDP exposure can lead to cellular and molecular changes associated with hepatic and renal tissue injury, with this deterioration being mediated by oxidative stress. These findings provide new details of the potential toxic effects of DIDP.

5. Conclusions

Collectively, the results from this study show that DIDP exposure can result in biochemical and histopathological alterations in the tissues of mice, which can lead to liver and kidney damage. Treatment with Vitamin E after DIDP exposure can reduce the oxidative damage induced by DIDP in mice. Our data suggest that oxidative stress may be partially responsible for the observed DIDP-induced toxicity. However, a deeper understanding of the molecular mechanisms of DIDP-induced liver and kidney damage require further study.

Declaration of interests

The authors declare that they have no known competing financial interests or personal relationships that could have appeared to influence the work reported in this paper.

Acknowledgements

This work was funded by the Hubei Province Health and Family Planning Scientific Research Project, China (Grant No. WJ2017Z027 and WJ2019M093), College Outstanding Young and Middle-aged Innovative Research Team Project of Hubei Province, China (Grant No. T201717).

References

Barcelos, R.P., Royes, L.F., Gonzalezgallego, J., et al., 2017. Oxidative stress and inflammation: liver responses and adaptations to acute and regular exercise. Free Radic. Res. 51 (2), 222–236.
Binnenmars, S.H., Hijmans, R.S., Navis, G., et al., 2017. Biomarkers of renal function: towards clinical actionability. Clin. Pharmacol. Ther. 102 (3), 481–492.
Bradley, E.L., Burden, R.A., Leon, I., et al., 2013. Determination of phthalate diesters in foods. Food Addit. Contam. A 30 (4), 722–734.
Chen, L., Lan, Z., Lin, Q., et al., 2013. Polydatin ameliorates renal injury by attenuating oxidative stress-related inflammatory responses in fructose-induced urate nephropathic mice. Food Chem. Toxicol. 52, 28–35.
Chen, X., Xu, S., Tan, T., et al., 2014. Toxicity and estrogenic endocrine disrupting activity of phthalates and their mixtures. Int. J. Environ. Res. Public Health 11, 3156–3168.
Cho, W.S., Han, B.S., Ahn, B., et al., 2008. Peroxisome proliferator diisodecyl phthalate has no carcinogenic potential in Fischer 344 rats. Toxicol. Lett. 178 (2), 110–116.
Cho, W., Jeong, J., Choi, M., et al., 2011. 26-Week carcinogenicity study of di-isodecyl phthalate by dietary administration to CB6F1-rasH2 transgenic mice. Arch. Toxicol. 85 (1), 59–66.
Choudhary, G.S., Alharbi, S., Almasan, A., 2015. Caspase-3 Activation is a critical determinant of genotoxic stress-induced apoptosis. Methods Mol. Biol. 1219, 1–9.
Dimitrov, M., Nikolova, I., Benbasat, N., et al., 2011. Acute toxicity, antidepressive and mao inhibitory activity of mangiferin isolated from Hypericum aucheri. J. Biotechnol. Biotechnol. Eq. 25 (4), 2668–2671.
Draper, H.H., Hadley, M., 1990. Malondialdehyde determination as index of lipid peroxidation. Methods Enzymol. 186, 421–431.
Espinosadiez, C., Miguel, V.S., Mennerich, D., et al., 2015. Antioxidant responses and cellular adjustments to oxidative stress. Redox biology 6, 183–197.
Feng, M., Li, Y., Qu, R., et al., 2013a. Oxidative stress biomarkers in freshwater fish Carassius auratus exposed to decabromodiphenyl ether and ethane, or their mixture. Ecotoxicology 22 (7), 1101–1110.
Feng, M., Qu, R., Wang, C., et al., 2013b. Comparative antioxidant status in freshwater fish carassius auratus exposed to six current-use brominated flame retardants: a combined experimental and theoretical study. Aquat. Toxicol. 140–141, 314–323.
Feng, M., He, Q., Meng, L., et al., 2015. Evaluation of single and joint toxicity of perfluorooctane sulfonate, perfluorooctanoic acid, and copper to Carassius auratus using oxidative stress biomarkers. Aquat. Toxicol. 161, 108–116.
Giovanoulis, G., Bui, T., Xu, F., et al., 2018. Multi-pathway human exposure assessment of phthalate esters and DINCH. Environ. Int. 112, 115–126.
Halden, R.U., 2010. Plastics and health risks. Annu. Rev. Public Health 31, 179–194.
Hoekstra, L.T., De Graaf, W., Nibourg, G.A., et al., 2013. Physiological and biochemical basis of clinical liver function tests: a review. Ann. Surg. 257 (1), 27–36.
Jha, J.C., Banal, C., Chow, B.S., et al., 2016. Diabetes and kidney disease: role of oxidative stress. Antioxidants Redox Signal. 25 (12), 657–684.
Kasibhatla, S., Amarantemendes, G.P., et al., 2006. Staining of suspension cells with hoechst 33258 to detect apoptosis. CSH Protocols 3 pdb.prot4492.
Kransler, K.M., Bachman, A.N., McKee, R.H., 2013. Estimates of daily di-isodecyl phthalate (DIDP) intake calculated from urinary biomonitoring data. Regul. Toxicol. Pharmacol 65, 29–33.
Lebel, C.P., Ischiropoulos, H., Bondy, S.C., 1992. Evaluation of the probe 2', 7'-dichlorofluorescin as an indicator of reactive oxygen species formation and oxidative stress. Chem. Res. Toxicol. 5 (2), 227–231.
Ma, P., Wu, Y., Zeng, Q., et al., 2013. Oxidative damage induced by chlorpyrifos in the hepatic and renal tissue of Kunming mice and the antioxidant role of vitamin E. Food Chem. Toxicol. 58, 1771–1783.
Majhi, C.R., Khan, S., Leo, M.D.M., et al., 2011. Effects of acetaminophen on reactive oxygen species and nitric oxide redox signaling in kidney of arsenic-exposed rats. Food Chem. Toxicol. 49, 974–982.
Morse, P.M., 2011. Phthalates face murky future. Chem.eng.news 89 (22), 28–31.
Nian, M., Li, Q., Bloom, M., et al., 2019. Liver function biomarkers disorder is associated with exposure to perfluoroalkyl acids in adults: isomers of C8 Health Project in China. Environ. Res. 172, 81–88.
Paradies, G., Paradies, V., Ruggiero, F.M., et al., 2014. Oxidative stress, cardiolipin and mitochondrial dysfunction in nonalcoholic fatty liver disease. World J. Gastroenterol. 20 (39), 14205–14218.
Patyna, P.J., Brown, R.P., Davi, R.A., et al., 2006. Hazard evaluation of diisononyl phthalate and diisodecyl phthalate in a Japanese medaka multigenerational assay. Ecotoxicol. Environ. Saf. 65 (1), 36–47.
Qin, W., Deng, T., Cui, H., et al., 2018. Exposure to diisodecyl phthalate exacerbated Th2 and Th17-mediated asthma through aggravating oxidative stress and the activation of p38 MAPK. Food Chem. Toxicol. 114, 78–87.
Rimessi, A., Previati, M., Nigro, F., et al., 2016. Mitochondrial reactive oxygen species and inflammation: molecular mechanisms, diseases and promising therapies. Int. J. Biochem. Cell Biol. 81, 281–293.
Saravanabhavan, G., Murray, J., 2012. Human biological monitoring of diisononyl phthalate and diisodecyl phthalate: a Review. J Environ Public Health 2012 810501.
Shen, S., Li, J., You, H., et al., 2017. Oral exposure to diisodecyl phthalate aggravates allergic dermatitis by oxidative stress and enhancement of thymic stromal lymphopoietin. Food Chem. Toxicol. 99, 60–69.
Valko, M., Rhodes, C.J., Moncol, J., et al., 2006. Free radicals, metals and antioxidants in oxidative stress-induced cancer. Chem. Biol. Interact. 160 (1), 1–40.
Wormuth, M., Scheringer, M., Vollenweider, M., et al., 2006. What are the sources of exposure to eight frequently used phthalic acid esters in europeans. Risk Anal. 26 (3), 803–824.
Wu, Y., Zhou, B.P., 2010. TNF-α/NF-κB/Snail pathway in cancer cell migration and invasion. Br. J. Canc. 102 (4), 639–644.
Yousef, M.I., Awad, T.I., Mohamed, E.H., 2006. Deltamethrin-induced oxidative damage and biochemical alterations in rat and its attenuation by Vitamin E. Toxicology 227 (3), 240–247.